Statistical models for carbon-nitrogen film growth

F. D. A. Aarão Reis and D. F. Franceschini
Instituto de Física, Universidade Federal Fluminense, Avenida Litorânea s/n, 24210-340 Niterói RJ, Brazil
(Received 21 July 1999)

We studied models of deposition and erosion, with two species of particles, that represent quantitatively many features of amorphous carbon-nitrogen film grown under plasma enhanced chemical vapor deposition. In the original model, the columns of the deposit are independent, and particles C and N are released with probabilities p and $1-p$, respectively. An incident C particle always aggregates upon contact with the surface. An N particle annihilates with a top C particle with probability q and aggregates with probability $1-q$. An N particle always annihilates with a top N. A critical line separates the regimes of growth ($p>q/2$) and erosion ($p<q/2$). For fixed q, when p decreases towards the critical value $p_c=q/2$, the bulk concentration of N (x_{N}) increases, and the growth rate r decreases. The $r\times x_{\mathrm{N}}$ curve for $q=0.25$ agrees with data from films grown in acetylene-nitrogen atmospheres. In order to represent the blocking of surface bonds by hydrogen atoms, we considered a second model in which any aggregation process is accepted with probability α, otherwise it is rejected. For $q=0.25$ and $\alpha=0.3$, the $r\times x_{\mathrm{N}}$ curve agrees with data from films grown in methane-nitrogen and methane-ammonia atmospheres. The fitting values of q and α were inferred from related experiments. In order to test the influence of lattice structure and spatial correlations, we also studied those models in simple cubic lattices, considering that the aggregation must satisfy the restricted solid-on-solid model conditions for the difference of heights in neighboring columns, while the erosion is random. We obtained similar results for $r\times x_{\mathrm{N}}$ curves, confirming the validity of those models to represent the kinetics of amorphous films growth. It was also observed that the surface roughness increases with x_{N}, which agrees qualitatively with several experiments on carbon-nitrogen films growth with ion bombardment.

PACS number(s): 05.40.−a, 05.70.Fh, 05.70.Ln, 68.55.−a

I. INTRODUCTION

The study of amorphous carbon-nitrogen (a-C:N) and hydrogenated carbon-nitrogen [a-C(N):H] films has attracted much interest in the last years [1]. Nitrogen incorporation was found to have beneficial effects on electrical [2], mechanical, and tribological [3–5] properties of amorphous carbon films. For instance, these films have improved performance as protective coatings compared to pure carbon films.

Most works in this field have been made using some kind of ion beam assistance. Plasma enhanced chemical vapor deposition (PECVD) in a hydrocarbon-nitrogen gas atmosphere [3,6], ionized reactive magnetron sputter deposition [5], dual ion beam deposition [7], and mass selected ion beam deposition (MSIBD) [8] should be mentioned among other techniques. An interesting feature of those processes is the rapid decrease of deposition rate when nitrogen incorporation increases [7,9], which limits the nitrogen content of the films. Depending on the deposition method, the maximum bulk nitrogen concentration ranges from 15 to 40%. These values, however, are well below the stoichiometric fraction of the compound β-C_3N_4, which was proposed to have mechanical properties compared to the ones of the crystalline diamond [10]. Another interesting feature of those films is the increase of surface roughness when nitrogen incorporation increases, which was already observed in the growth with several techniques [11,12].

In order to understand structure and properties changes induced by nitrogen incorporation in a-C(N) and a-C(N):H films, it is important to study the physics of the deposition process. This is a complex task if we consider the collision processes following ion subsurface penetration, from ion stopping to bond formation [13]. In fact, the microscopic properties of the growing surfaces of amorphous carbon-nitrogen films are not well understood yet.

Statistical models are interesting at this point since they may describe some aspects of the growth kinetics by representing the basic growth mechanisms as simple stochastic processes and neglecting the details of the microscopic interactions. Following this reasoning, here we will present simple models of aggregation and erosion that describe quantitatively some kinetic features of carbon-nitrogen film growth by PECVD. Instead of considering the microscopic details of the growing surfaces, these models are based on experimental information that can be treated statistically, such as deposition or etching rates and surface roughness (interface widths). Although this approach has a limited applicability, the statistical description of the competition between aggregation and erosion in carbon-nitrogen films growth is complementary, and may even be helpful to the study of microscopic models.

In a recent paper [14], we introduced a model of random deposition and erosion, with two species (C and N particles), that represents qualitatively the growth kinetics of carbon-nitrogen films deposited by PECVD, and agrees quantitatively with results of an experiment in acetylene-nitrogen atmospheres [15]. In that model, the incidence of nitrogen ions (each atom is represented by an N particle) is responsible for the erosion processes, which describe the evolution of CN and N_2 molecules.

The first aim of the present paper is to present the details of the solution of that model and discuss its consequences. Hereafter we will refer to it as the original model [14].

Our second aim is to generalize that model in order to

1063-651X/2000/61(4)/3417(9)/$15.00 © 2000 The American Physical Society

represent quantitatively the growth kinetics of a-C(N):H films by PECVD in different conditions. For this purpose, we will introduce a blocking of surface sites to aggregation. It represents the effects of hydrogen atomic radicals that, as a main rule, saturate surface dangling bonds [16], thus avoiding the aggregation of carbon-containing radicals and nitrogen atoms. This second model will also be solved analytically, and will represent growth properties of a-C(N):H films in methane-nitrogen and methane-ammonia atmospheres.

The values of the parameters of the models used to fit experimental data (parameters q and α) were inferred from independent experiments, in order to warrant the consistency of the theoretical approach. Finally, we will introduce surface relaxation mechanisms to the aggregation processes of the previous models, i.e., mechanisms to avoid the formation of huge hills or valleys at the surface. For this purpose, we will consider a three-dimensional lattice structure and a generalization of the conditions of the restricted solid-on-solid (RSOS) model [17,18] to the aggregation processes, while the erosion processes will be uncorrelated. Although these mechanisms are very far from the real surface kinetics, they are helpful to analyze the effects of lattice structure and surface relaxation on the previous models. We will show that the deposition rate versus nitrogen concentration curves have small differences from the corresponding uncorrelated models, i.e., they are weakly dependent on those mechanisms. It gives additional support to our comparisons with experimental data on amorphous films. We will also show that these models represent qualitatively the increase of surface roughness with nitrogen content, as observed experimentally.

This work is organized as follows. In Sec. II we will present the original model for random deposition and erosion of carbon-nitrogen films and its motivations. In Sec. III we review the analytic solution of that model, discuss its consequences and the comparison with PECVD experiments in acetylene-nitrogen atmospheres. In Sec. IV we will extend this model to include the blocking of surface sites to aggregation and show that it describes experimental results from deposition in atmospheres with methane. In Sec. V we will introduce a lattice structure and surface relaxation mechanisms in the aggregation processes of the original model, and analyze their effects on growth rates, concentrations of C and N and surface roughness. In Sec. VI we will introduce the same mechanisms in the model with blocking of surface sites. In Sec. VII we summarize our results and conclusions.

II. THE ORIGINAL MODEL OF RANDOM DEPOSITION AND EROSION

In amorphous carbon-nitrogen or hydrogenated carbon-nitrogen films growth, the observed fall in deposition rate has been ascribed to the onset of a chemical sputtering process upon increasing nitrogen flux towards film surface [7,19]. This process was studied in detail by Hammer and Gissler [20], who measured the mass spectrum of the evolved molecules from a pure graphite sample submitted to low energy N_2^+ ion bombardment. They observed that film erosion occurs as a kind of chemical sputtering, which results in the evolution of CN molecules, with a carbon etch rate of about 0.5 C atoms per N_2^+ ion. In a recent work, Hong and Turban [21] also observed the chemical sputtering of a-C:H films by low energy N_2^+ ions coming from a N_2 plasma. The evaporation of N_2 molecules, as a consequence of N-N bond formation during the growth, may also contribute to the erosion process, as suggested by Marton *et al.* [1]. There is no experimental evidence on the presence of N-N bonds in carbon-nitrogen films, and recent molecular dynamics simulations of the formation of carbon-nitrogen solids [22] have shown evaporation of N_2 at high nitrogen incorporation rates.

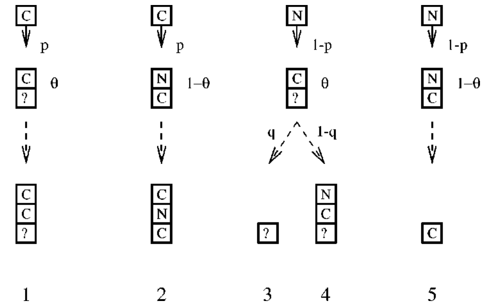

FIG. 1. Processes following the incidence of a particle (squares) at a column. The question mark indicates particles that may be C or N. The probabilities associated to a given incident particle (p or $1-p$), a top particle (θ or $1-\theta$) and an erosion process (q or $1-q$) are also shown.

This scenario suggested the existence of aggregation and erosion processes in carbon-nitrogen films growth by PECVD and other techniques with ion beam assistance. It motivated the introduction of a model for random deposition and erosion with two species, C and N [14]. In this model, the substrate columns are independent, consequently the deposition process may be analyzed as a single column process [a (0+1)-dimensional model]. The incident flux contains a fraction p of C particles and a fraction $1-p$ of N particles. The C particles represent carbon-carrying species (fast ions or slow neutral radicals) that come from the plasma and effectively stick to the film surface. The N particles represent the products of the bond breaking of N_2^+ fast ions after colliding with the surface.

Figure 1 shows the effects of the incidence of each particle on a column of the aggregate. A C particle is deposited whatever the top particle is (processes 1 and 2). An incident N particle may annihilate with a top C particle with probability q (process 3), and deposits over it with probability $1-q$ (process 4). This annihilation (erosion) process represents the evaporation of CN molecules after the incidence of a nitrogen ion. The probability q is related to the interactions between the incident nitrogen ions and the aggregated carbon atoms. Finally, the incident N annihilates a top N particle with probability 1 (process 5). It represents the evaporation of N_2 and the absence of N-N bonds in the films. θ is the fraction of C particles at the surface (top of the columns), thus the probability of any particle falling over a C is θ, while the probability of falling over an N is $1-\theta$. If the top particle of the column is C, then the particle below it is not known a priori (particles labeled with a question mark). If the top particle is N, then the particle below it is certainly a C, because process 5 do not allow consecutive N particles in a column.

The random deposition is the simplest statistical growth

model [27,25]. It has already been studied with one or two kinds of particles [28] but erosion processes do not seem to have been previously introduced. Despite its simplicity, a random deposition model is the first step towards correlated models, which give more realistic descriptions of surface roughening and which are widely discussed in the recent literature [23–26].

The present model and its further extensions (Secs. IV, V, and VI) are statistical descriptions of the essential aspects of carbon-nitrogen film growth kinetics which avoid the complications of the microscopic interactions in the film surface. Consequently, they do not represent properties intimately related to the film structure. Other important assumptions of this statistical description are discussed below.

First, we are assuming that nitrogen incorporation and nitrogen or carbon erosion processes are carried out mainly by N_2^+ ions that impinge on the growing surface and break into two N atoms of about half of the initial ion energy. We are also neglecting the role of fast carbon ions in the removal of nitrogen atoms from the film—the symmetric situation to process 4 in Fig. 1. Despite the key role played by the carbon-carrying fast ions in *a*-C:H film growth process [29], the major contribution to the growth rate has been shown to come from carbon-carrying radicals [30], and it is expected that these features generalize to films containing nitrogen.

Finally, we are also neglecting the role played by hydrogen ions and radicals in the film growth. According to Jacob [16], the dominant effect of hydrogen close to room temperature is to decrease the number of dangling bonds at the surface. Since carbon-carrying radicals or slow nitrogen atoms (resulting from the breaking of fast N_2^+ ions) may aggregate at these dangling bonds, we are neglecting the blocking of surface sites to C and N species bonding in the original model. In Sec. IV, we will show that this blocking must be considered in order to represent the growth kinetics of PECVD films in hydrogen-rich atmospheres.

III. ANALYTIC SOLUTION OF THE ORIGINAL MODEL FOR RANDOM DEPOSITION AND EROSION

In this model, there is no correlation between different columns. However, C and N particles are not symmetric, then the growth at a given time depends on the history of the growth process. An exact solution of the problem is difficult, except if we just consider the asymptotic behavior.

The number of deposited C particles (n_C), at a given time t, varies as

$$r_C \equiv \frac{dn_C}{dt} = p-(1-p)\theta q. \tag{1}$$

The first term (p) of Eq. (1) is the contribution from processes 1 and 2 (Fig. 1), and the second term $[(1-p)\theta q]$ is the contribution from process 3. One unit of time is assigned to each attempt to aggregate or to annihilate one particle. The number of deposited N particles (n_N), at a given time t, varies as

$$r_N \equiv \frac{dn_N}{dt} = (1-p)\theta(1-q)-(1-p)(1-\theta). \tag{2}$$

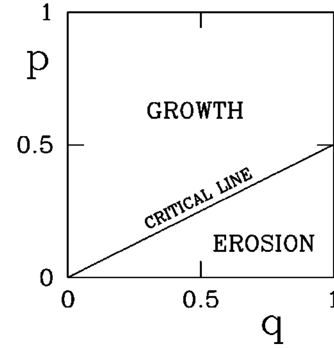

FIG. 2. Diagram of the three possible regimes of the model. At the critical line, the C and N deposition rates are zero.

The first term $[(1-p)\theta(1-q)]$ of Eq. (2) is the contribution from process 4 and the second term $[(1-p)(1-\theta)]$ is the contribution from process 5. In Eqs. (1) and (2), θ represents the coverage at time t (probability of a top C particle).

Those processes may also lead to changes in the coverage θ. The fraction of C particles at the surface after the annihilation process 3 (particles labeled with a question mark) is the only unknown value in Fig. 1. The particle labeled with a question mark was at the second layer (from top to bottom), below a C particle, before the erosion process 3. If the removed C particle was deposited at time t_1 ($t_1<t$), then the probability of "?" being a C particle is $\theta(t_1)$. Thus we obtain

$$\theta(t+1) = p+(1-p)\theta(t)q\theta(t_1)+(1-p)[1-\theta(t)]. \tag{3}$$

The first term in Eq. (3) (p) is the contribution from processes 1 and 2, the second term $[(1-p)\theta(t)q\theta(t_1)]$ is the contribution from process 3 and the third term $\{(1-p)[1-\theta(t)]\}$ is the contribution from process 5.

In the stationary growth regime, $\theta(t+1)=\theta(t)=\theta(t_1)$. Then Eq. (3) gives the asymptotic coverage θ as function of p and q:

$$\theta = \frac{2-p-\sqrt{(2-p)^2-4q(1-p)}}{2q(1-p)}. \tag{4}$$

Substitution in Eqs. (1) and (2) gives the stationary rates

$$r_C = \frac{3}{2}p-1+\frac{1}{2}\sqrt{(2-p)^2-4q(1-p)}, \tag{5}$$

$$r_N = \frac{(2-q)}{2q}\left[2-p-\sqrt{(2-p)^2-4q(1-p)}\right]-1+p. \tag{6}$$

There is a transition between the regimes of growth and erosion at the critical line $p=q/2$, where $r_C=r_N=0$ (Fig. 2). Above the critical line, the numbers of deposited particles n_C and n_N increase with time. Below that line, any initial aggregate will be destroyed, due to the high number of incident N particles and the high probability of annihilating with C particles.

In the growth regime, for fixed q, the total growth rate (or growth velocity) $r=r_C+r_N$ decreases as p decreases towards $p_c=q/2$. The numbers of deposited particles in the long time

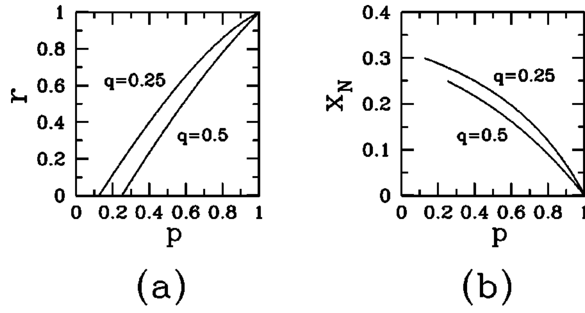

FIG. 3. (a) Growth rate r versus the probability p of incidence of C particles in the growth regime, for $q=0.25$ and $q=0.5$; (b) Bulk concentration x_N of N particles versus p, for the same values of q.

limit are $n_C=r_Ct$ and $n_N=r_Nt$, and the total number of particles is $n=n_C+n_N$. Then the bulk concentrations of C and N are $x_C\equiv n_C/n=r_C/(r_C+r_N)$ and $x_N\equiv n_N/n=r_N/(r_C+r_N)$.

In Fig. 3(a) we show r versus p in the growth regime for $q=0.25$ and $q=0.5$, obtained from Eqs. (5) and (6), and in Fig. 3(b) we show the concentration x_N for the same values of q. We observe that, as p decreases, r decreases and x_N increases. The dependence of r and x_N on p are qualitatively the same for all q.

x_N has a maximum limiting value

$$x_N^{(c)}=\lim_{p\to p_c^+} x_N=\frac{(1-q)}{(3-2q)} \tag{7}$$

as the critical point is approached. For $q=0$, $x_N^{(c)}=1/3$, which is the maximum possible concentration of N particles in this model. For $q=0.25$, $x_N^{(c)}=0.3$ [Fig. 3(b)]. It is interesting that this maximum is attained when the annihilation processes are more frequent and the growth is very slow. It agrees with the experimental observations of decrease of deposition rate as the nitrogen incorporation increases. It can also be shown that the concentration of N particles at the surface $(1-\theta)$ is always larger than the concentration of N particles in the bulk.

In order to compare our model and experimental results, it is convenient to plot the deposition rate r versus the nitrogen concentration x_N. In Fig. 4 we show the $r\times x_N$ curves for $q=0$, 0.25, 0.5, and 0.75. For $q\lesssim 0.5$, the downward curvature reproduces the behavior of the growth rate observed in experiments [6,7,15,31].

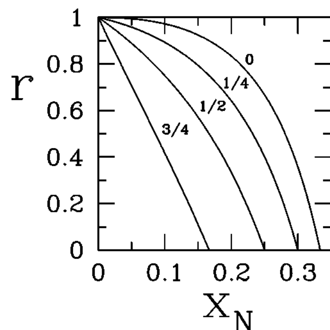

FIG. 4. Growth rate r versus bulk concentration x_N of N particles for the indicated values of q.

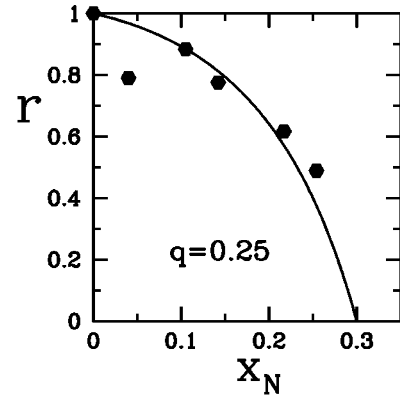

FIG. 5. Growth rate r versus bulk concentration x_N of N particles of the original model with $q=0.25$ (solid line), and experimental results for films grown in acetylene-nitrogen atmospheres (hexagons, Ref. [15]).

The present model describes quantitatively the results reported by Jacobsohn *et al.* [15] on the growth kinetics of hydrogenated carbon-nitrogen films grown under PECVD in acetylene-nitrogen atmospheres. In Fig. 5 we show the growth rate r as a function of x_N, for $q=0.25$, and we also show the relative deposition rate of Ref. [15] as a function of the concentration of nitrogen (at. %) in the films. The experimental concentrations presented here were obtained from the ammounts of C and N only, excluding the hydrogen content, which is near 10%. It is reasonable for a comparison with a model that considers only C and N atoms, as discussed in Sec. II.

The value $q=0.25$ was inferred from the 0.5 C atom per N_2^+ ion removal ratio reported by Hammer and Gissler [20]. Thus our description is consistent with data taken from independent experiments and did not use arbitrary fitting parameters.

The main limitation of this model is the absence of spatial correlations. In Sec. V, this limitation will be partly overcome with the introduction of a lattice structure and surface relaxation, but keeping the same probabilistic rules to select aggregation or erosion processes. We will show that these ingredients do not have remarkable effects on the $r\times x_N$ curves (such as that in Fig. 5), which confirms the validity of our comparisons with experimental data on amorphous films.

The deposition rate curves reported for PECVD using other hydrocarbons, such as methane, have similar shapes to the $q=0.25$ curve of this model, but the maximum of x_N ranged from 13 to 15 at. %. These values of $x_N^{(c)}$ are obtained in the original model with $q>0.75$. However, the curve for $q>0.75$ (see the trend in Fig. 4) is completely different of the experimental ones, which always have a downward curvature. The behavior in acetylene-nitrogen atmospheres is probably due to the less easy dissociation of acetylene in the plasma [32]. Using other hydrocarbons, the plasma dissociation products, such as hydrogen radicals and ions, may also play a role in the film growth process. In Sec. IV, we will show how the blocking of surface sites to aggregation properly represent these experiments.

IV. MODEL WITH BLOCKING OF SURFACE SITES

The original model discussed in Secs. II and III is not able to represent quantitatively the $r\times x_N$ curves with $x_N^{(c)}\approx 0.15$,

such as those with methane in the plasma. These results suggest that the abundance of hydrogen in the plasma has an important effect on deposition rates and nitrogen incorporation, a feature that was not considered in the original model.

The higher hydrogen content in the plasma and the easier dissociation of CH_4, compared to C_2H_2, increase the flux of hydrogen ions and radicals towards film surface. As discussed in Sec. II, the main role of hydrogen is to decrease the number of dangling bonds at the surface, thus decreasing the aggregation probability. Results from deposition of nitrogen-free films are helpful at this point: it is observed that the deposition in acetylene atmospheres [33] is remarkably faster than the deposition in methane atmospheres [34] for the same bias voltage and pressure. For a large variety of growth conditions, the ratio of deposition rates ranges approximately from 2 to 6 [33,34]. For instance, using a -300 V self-bias, Zou *et al.* [33] obtained approximately the deposition rate 400 Å/min with $p_{C_2H_2}=5.2\times10^{-2}$ mbar and the deposition rate 100 Å/min for $p_{CH_4}\approx5\times10^{-2}$ mbar.

This scenario suggests the introduction of a blocking factor in the original model, in order to represent the saturation of surface bonds and, consequently, the decrease of the aggregation probability in a plasma with methane. Therefore we will consider that the aggregation processes of Fig. 1 (processes 1, 2, and 4) are accepted with a probability α, otherwise they are rejected. When rejected, neither aggregation nor erosion occurs. On the other hand, the erosion processes 3 and 5 are always accepted.

In the case $p=1$ (only C particles), the absolute deposition rate in this model is α times the deposition rate in the original model. The comparison above between deposition rates in acetylene and methane atmospheres suggests α ranging between $1/6\approx0.17$ and $1/2=0.5$ to model deposition in methane atmospheres, since the original model represented the deposition in acetylene atmospheres.

In the present model, Eqs. (1) and (2) are replaced by

$$r_C\equiv\frac{dn_C}{dt}=\alpha p-(1-p)\theta q \tag{8}$$

and

$$r_N\equiv\frac{dn_N}{dt}=\alpha(1-p)\theta(1-q)-(1-p)(1-\theta). \tag{9}$$

Equation (3) is replaced by

$$\theta(t+1)=p\theta(t)+\alpha p[1-\theta(t)]+(1-p)\theta(t)q\theta(t_1)+(1-\alpha)(1-p)\theta(t)(1-q)+(1-p)[1-\theta(t)], \tag{10}$$

also with $t<t_1$.

The asymptotic condition $\theta(t+1)=\theta(t)=\theta(t_1)$, when applied to Eq. (10), gives θ as function of p, q, and α, analogously to Eq. (4). Substitution in Eqs. (8) and (9) gives r_C and r_N as functions of those parameters, analogously to Eqs. (5) and (6).

In the $pq\alpha$ space, there is a critical surface separating the regimes of growth ($r_C>0$, $r_N>0$) and erosion ($r_C<0$, $r_N<0$), whose equation is

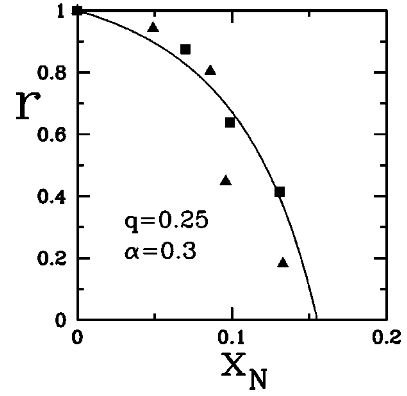

FIG. 6. Relative growth rate r versus bulk concentration x_N of N particles of the model with blocking of surface sites with $q=0.25$ and $\alpha=0.3$ (solid line) and experimental results for films grown in methane-nitrogen (squares, Ref. [3]) and methane-ammonia (triangles, Ref. [11]) atmospheres. Theoretical and experimental growth rates were normalized to give $r_{max}=1$ (for nitrogen-free films).

$$p=p_c=\frac{q}{\alpha^2(1-q)+\alpha+q}. \tag{11}$$

The growth regime is obtained for $p>p_c$. In this regime, for fixed q and α, we observe that r decreases when p decreases, while x_N increases, such as in Fig. 3.

From Eqs. (8) and (9), the maximum value of r in this model is α (for $p=0$). However, in our comparisons of theoretical and experimental deposition rates, they will be normalized to give $r_{max}=1$ (nitrogen-free films). We will consider the same value $q=0.25$ used to describe experiments in acetylene atmospheres (Sec. III) and suggested by an independent work [20]. The best fit of the $r\times x_N$ curves of films grown in methane-nitrogen [3] and methane-ammonia [11] atmospheres is obtained with $\alpha=0.3$, as shown in Fig. 6. The corresponding critical point ($r=0$) is at $p_c\approx0.4048\cdots$. The experimental values of x_N are obtained only from the ammounts of carbon and nitrogen in the films, as discussed above.

We note the good agreement between the model and the data from two different experiments, which lay approximately in the same curve. The blocking of surface sites to aggregation provides, at the same time, a faster decrease of deposition rates and lower nitrogen concentrations. It is also important to stress that the value of the free parameter $\alpha=0.3$ is consistent with the typical ratios of absolute deposition rates in methane and acetylene atmospheres, as discussed above.

V. THE ORIGINAL MODEL WITH SURFACE RELAXATION

The models presented in the previous sections neglected spatial correlations. An important point if we intend to model real films is the relevance of the three-dimensional structure and of those correlations. For instance, it is important to know their effects on the $r\times x_N$ curves presented above, and the influence of nitrogen incorporation in surface roughness.

These questions motivated the introduction of some simple mechanisms of surface smoothing to the aggregation

processes presented above. The simplification of the film structure and of the mechanisms of surface roughening, as well as the previous approximations of the uncorrelated models, indicate that we cannot expect more than qualitative information in addition to the results presented before. Quantitative information on surface roughness, for instance, would be possible only if the amorphous structure of the films and the details of the interactions between the plasma and the films' surfaces were taken into account.

In our first model with surface relaxation, we will consider that the deposit has a simple cubic lattice structure, and that the aggregation and erosion processes have the same probabilities of Fig. 1 (parameters p and q). The substrates are square lattices (xy plane) of widths $L=16$, 32, and 64. Periodic boundaries are adopted in the x and y directions.

We will generalize the well-known restricted solid-on-solid (RSOS) model [17,18] to the aggregation processes of Fig. 1 (processes 1, 2, and 4). It forbids the formation of hills or valleys of heights larger than one lattice parameter. More precisely, we will consider a version of this model that resembles the modified RSOS model of Kim *et al.* [18]. The incident particle (C or N) and the aggregation or erosion process (1 to 5) are selected with the same probabilities p and q, as described in Sec. II (Fig. 2), considering only the top particle of the column of incidence. If it is decided to aggregate the incident particle (processes 1, 2, or 4), we look at the four neighboring columns to find whether their heights are larger than or equal to the height of the column of incidence. In the positive case, the aggregation process is accepted. Otherwise, a neighboring column is randomly chosen, the test of neighboring columns' heights is performed and, if it is positive, the aggregation is accepted. This procedure is repeated until it is found a column where the aggregation is accepted. Figure 7 shows examples of aggregation processes in a two-dimensional version of the model.

On the other hand, when an erosion process is chosen (according to the probabilities of the original model), the top particle of the column of incidence is removed. Thus the erosion may form hills or valleys of heights larger than one, while the aggregation tends to keep the surface locally smooth. This is reasonable as a first approximation, although the actual sputtering processes may lead to the formation of patterns at the surface that are described by much more complex models [35].

We simulated the deposition of films up to 5×10^6 particles. This number is sufficient to attain the regime of roughness saturation in lattices with $L=16$ and $L=32$. For fixed $q=0.25$, we simulated the deposition for several values of p, with intervals $\Delta p=0.1$. A total of 2×10^3 deposits were generated for each pair (p,q) and each lattice width L.

In Fig. 8 we show the deposition rate r versus inverse time $1/t$ (one unit time is assigned to each attempt to deposit or to remove one particle), for $q=0.25$ and $p=0.6$, in the three lattices. Note the small range of the vertical axis in Fig. 8, which provides very accurate estimates of asymptotic deposition rates. The asymptotic deposition rate for lattice width L, r_L, is obtained from extrapolations to $t\rightarrow\infty$ ($1/t\rightarrow0$). This extrapolation method was previously applied to the original model and the results agree with the analytic solution with a very high accuracy (nearly 1 part in 10^5). The estimates r_L are then extrapolated to $L\rightarrow\infty$ to give the final estimate of the deposition rate r. For instance, for $p=0.25$ and $q=0.6$ (Fig. 8), the final estimate is $r=0.65945\pm0.00010$. Similar extrapolation procedure is used to calculate the asymptotic fraction of N particles x_{N}.

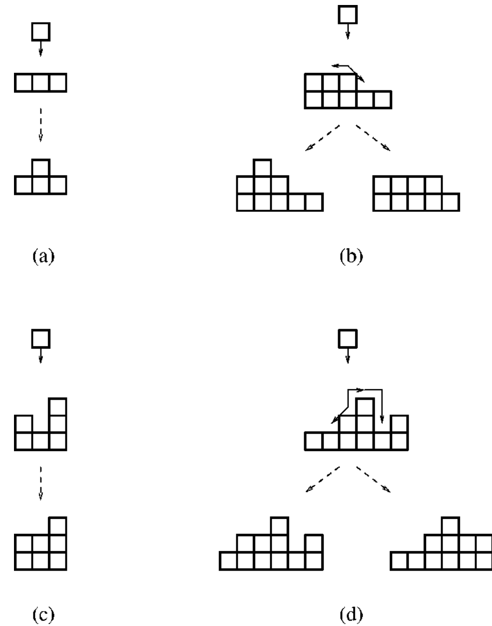

FIG. 7. Examples of aggregation of particles in the models with surface relaxation (two-dimensional version). Solid arrows indicate the steps of the incident particle when it is choosing a column to aggregate. Dashed arrows indicate the deposits that may be obtained after the aggregation of the incident particle [two possible final deposits in cases (b) and (d)].

In Fig. 9 we show r versus x_{N} for the present model and the curve for the original model, both with $q=0.25$. The data of Ref. [15] for a-C(N):H films grown under PECVD in acetylene-nitrogen atmospheres (same as Fig. 6) is also shown in Fig. 9.

We note that the introduction of surface smoothing mechanisms do not change remarkably the deposition rates and concentrations when compared to the random model for $x_{\mathrm{N}}<0.25$. Simulations for other values of q confirm this behavior. The differentiated behavior for larger x_{N} is expected because, in the present model, it is possible the deposition of consecutive N particles in a certain column; it occurs when

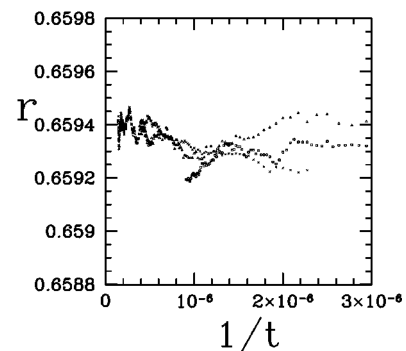

FIG. 8. Deposition rate r versus inverse growth time $1/t$, in the original model with surface relaxation, for $q=0.25$, $p=0.6$ and three lattice widths: $L=16$ (squares), $L=32$ (triangles), and $L=64$ (crosses).

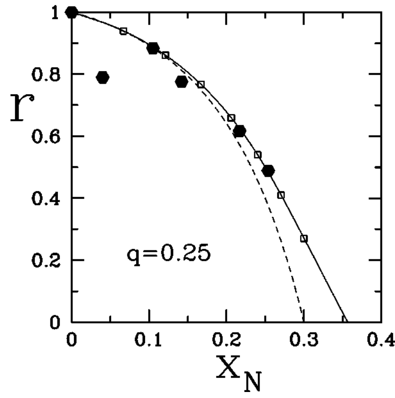

FIG. 9. Growth rate r versus bulk concentration x_N of N particles. Empty squares are results of simulations of the original model with surface relaxation, with $q=0.25$, and the solid curve is a fit of those data. The dashed curve is the analytic result of the original model (uncorrelated) with $q=0.25$. Full hexagons are experimental results for films grown in acetylene-nitrogen atmospheres (Ref. [15]).

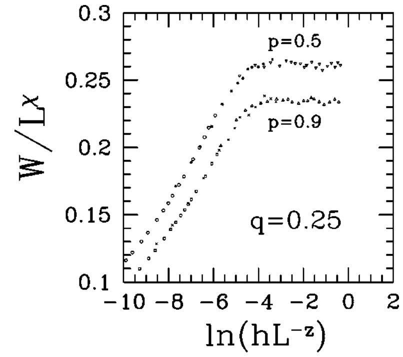

FIG. 10. Scaling plot of the interface width W versus average film height h of the original model with surface relaxation, with $q=0.25$ and the values of p indicated. Critical exponents are $\chi=0.55$ and $z=3.1$. Lattice widths are $L=16$ (up and down triangles), $L=32$ (crosses and stars), and $L=64$ (squares and hexagons). The N particle concentration increases when p decreases.

the upper N did not incide at that column, but aggregated in it (as shown in Fig. 7). When x_N is small, this event has a very low probability.

We conclude that the essential ingredients of the model give deposition rates and concentrations that weakly depend on the lattice structure and the surface relaxation mechanisms for $x\lesssim0.25$. These results give additional support to our comparisons with experimental data from amorphous films, whose structure and deposition mechanisms are much more complex. It proves that the model captured the relevant statistical properties of the film growth kinetics, avoiding the complexities of the microscopic interactions.

On the other hand, the surface morphology certainly depends on lattice structure and surface relaxation mechanisms. Although these ingredients are very far from the real ones in plasma deposition, it is interesting to study the surface morphology because it gives qualitative information on the variation of surface roughness with the conditions of deposition and also to provide a more complete analysis of the theoretical model.

The interface width, which measures surface roughness, is defined as

$$W=\left[\frac{1}{L^2}\sum_i\left(\langle h_i^2\rangle-\langle h_i\rangle^2\right)\right]^{1/2}, \qquad (12)$$

where h_i is the height of column i.

For fixed p and q, we expect that W obeys the scaling relation

$$W\approx L^\chi f(Lh^{-1/z}), \qquad (13)$$

where f is a scaling function and h is the mean height of the deposit $[h=(n_C+n_N)/L^2]$. When erosion is absent, h is a measure of the deposition time per substrate site. When erosion processes work, scaling plots are useful to compare the surface roughness of films with the same mean height (which, however, need different times to attain that height).

In Fig. 10 we show W/L^χ versus $\ln(hL^{-z})$, using $\chi=0.55$ and $z=3.1$, for ($q=0.25$, $p=0.9$) and ($q=0.25$, $p=0.5$). The corresponding deposition rates are $r\approx0.94$ and $r\approx0.54$ (Fig. 9). The exponents χ and z provide the best data collapse for the three lattice widths L.

It is clear that the roughness increases when p decreases and x_N increases, if films with the same mean height h are compared. The uncorrelated erosion processes, which are more frequent when the N flux increases, are responsible for this feature. However, it is interesting to note that the dominant aggregation processes lead to a saturation of the interface width, such as in the correlated models without erosion.

VI. MODEL WITH BLOCKING OF SURFACE SITES AND SURFACE RELAXATION

Now we generalize the model presented in Sec. IV, considering the blocking of surface sites to aggregation and surface relaxation mechanisms. The attempts to aggregate a particle (processes 1, 2, and 4) are accepted with probability α, otherwise they are rejected. The aggregation, when accepted, obeys the same (RSOS like) conditions presented in Sec. V, with the same procedure to choose the column for the aggregation (Fig. 7). The erosion is random and is always accepted, such as in the previous models.

We simulated the present model in lattices with widths $L=16$, 32, and 64, for $q=0.25$ and $\alpha=0.3$. In Fig. 11 we show r versus x_N for this model (r was normalized to give $r_{max}=1$). We also show the same data of Fig. 6: the curve for the uncorrelated model with blocking of surface sites (Sec. IV) and the data from a-C(N):H films grown under PECVD in methane-nitrogen [3] and methane-ammonia [11] atmospheres. We observe that the introduction of a lattice structure and surface smoothing mechanisms do not change remarkably the $r\times x_N$ curves up to $x_N\approx0.12$. It reinforces our comparisons with experimental data in amorphous films. The differentiated behavior for larger x_N is explained as in the previous model.

In Fig. 12 we show W/L^χ versus hL^{-z}, using $\chi=0.55$ and $z=3.1$, for ($q=0.25$, $\alpha=0.3$, $p=1$) and ($q=0.25$, $\alpha=0.3$, $p=0.6$). The absolute deposition rates are $r=0.3$ and $r\approx0.11$, respectively (relative deposition rates $r=1$ and $r\approx0.37$ - Fig. 11).

The exponents $\chi=0.55$ and $\chi=3.1$ give the best data col-

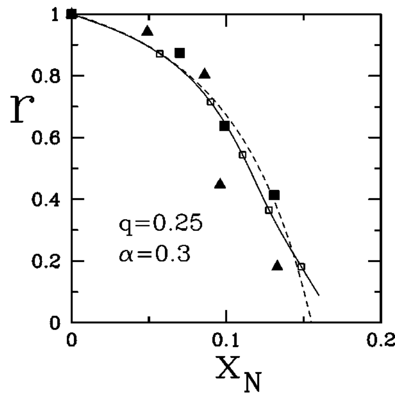

FIG. 11. Relative growth rate r versus bulk concentration x_N of N particles. Empty squares are results of simulations of the model with blocking of surface sites and surface relaxation, with $q=0.25$ and $\alpha=0.3$, and the solid curve is a fit of those data. The dashed curve is the analytic result of the uncorrelated model with blocking of surface sites, with the same values of q and α. Full squares and triangles are experimental results for films grown in methane-nitrogen (Ref. [3]) and methane-ammonia (Ref. [11]) atmospheres, respectively. Growth rates are normalized to give $r_{max}=1$.

lapse for $p=1$ (films with no N particle). The best data collapse for $p=0.6$ is obtained with slightly different values of χ and z. It is probably an effect of corrections to scaling, since the aggregation and the erosion mechanisms belong to different universality classes. It is also interesting to note that the exponents do not change with the introduction of the blocking of surface sites to aggregation.

In this model, we also observe the increase of roughness when p decreases and x_N increases. It agrees with the results of Priolli *et al.* [11], who measured the surface texture of films grown in methane-ammonia atmospheres with atomic force microscopy techniques. In that experiment, the surface width doubles ($0.13\rightarrow0.26$ nm) when the relative deposition rate falls from 1 (nitrogen-free films) to 0.41 ($x_N\approx0.135$, considering only the ammounts of carbon and nitrogen). Films with the same thickness (about 35 nm) were analyzed.

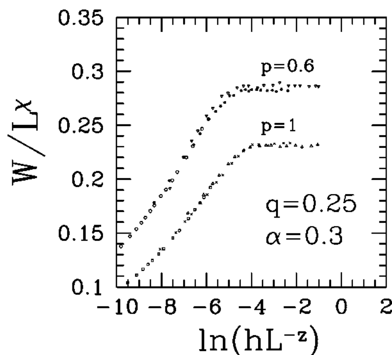

FIG. 12. Scaling plot of the interface width W versus average film height h of the model with blocking of surface sites and surface relaxation, with $q=0.25$, $\alpha=0.3$, and the values of p indicated. Critical exponents are $\chi=0.55$ and $z=3.1$. Lattice widths are $L=16$ (up and down triangles), $L=32$ (crosses and stars) and $L=64$ (squares and hexagons). The N particle concentration increases when p decreases.

In our model, the interface width increases by a smaller factor (nearly 25%) from $p=1$ to $p=0.6$. The uncorrelated erosion processes, that become more frequent when the nitrogen concentration increases, are responsible for the increase of surface roughness. Since the lattice structure of our model is very distant from the real films structure and the surface smoothing mechanisms are somewhat artificial, we do not expect more than a qualitative agreement. A quantitative comparison would require a much more sophisticated model, taking into account the complex geometry of the deposit and the interactions with the plasma, which is far from the present knowledge of those deposition processes.

VII. SUMMARY AND CONCLUSION

We presented models of deposition and erosion, with two species (C and N), which represent many features of plasma deposited amorphous carbon-nitrogen films. In these models, the incidence of N particles is responsible for the erosion. In the original version of the model [14], the probability of incidence of a C particle is p and the probability of an incident N particle annihilating an aggregated C particle is q. In the second version, there is a probability α of accepting the aggregation attempt ($\alpha=1$ in the original model). It represents the blocking of surface sites to the aggregation, which is typical of hydrogen-rich plasmas. We also studied these models including surface smoothing mechanisms (generalizations of the RSOS model [17]) in the aggregation processes.

For the random deposition and erosion models, we calculated analytically the deposition rates and C and N concentrations as functions of p, q and α. The $r\times x_N$ curve of the original model with $q=0.25$ agrees with experimental data from amorphous carbon-nitrogen films grown in acetylene-nitrogen atmospheres. The $r\times x_N$ curve of the model with blocking of surface sites, with $q=0.25$ and $\alpha=0.3$, agrees with the data from films grown in methane-nitrogen and methane-ammonia atmospheres. Those values of q and α are consistent with independent experiments on growth or erosion of nitrogen-free films [20,33,34]. The models with surface relaxation were studied using numerical simulations. The $r\times x_N$ curves of these models have small differences from the corresponding curves of the uncorrelated models in the range of x_N that agrees with experimental data. It proves that those curves are weakly dependent on lattice structure and surface relaxation mechanisms, which supports our comparisons with data from amorphous films.

The models with surface relaxation mechanisms for the aggregation have also shown an increase of surface roughness when the nitrogen concentration increased. It is a consequence of the absence of correlations in the erosion processes, which become more frequent when the N flux increases and, consequently, x_N increases. These features are also observed in real films deposited by different techniques with ion bombardment.

Although our models do not consider the microscopic details of film growth, the statistical point of view may be useful for the interpretation of related experiments where deposition and erosion simultaneously occur. For instance, transitions between the growth and erosion regimes are observed in other thin film growth problems, such as a-C:H

films [16] when the substrate temperature increases. From a theoretical point of view, it would also be interesting the investigation of the points where aggregation and erosion are balanced out ($r=0$), when these processes belong to different universality classes. Thus we consider that further studies of models of deposition and erosion may be motivated by the present work. Moreover, we hope that our models will help future studies focusing on the microscopic properties of amorphous carbon or carbon-nitrogen films deposited by plasma.

ACKNOWLEDGMENTS

This work was partially supported by CNPq and FINEP (Brazilian agencies).

[1] D. Marton, K.J. Boyd, and J. W. Rabalais, Int. J. Mod. Phys. B **9**, 3527 (1995).

[2] S.R.P. Silva, J. Robertson, G.A.J. Amaratunga, B. Raferty, L.M. Brown, D.F. Franceschini, and G. Mariotto, J. Appl. Phys. **81**, 2626 (1997).

[3] D.F. Franceschini, C.A. Achete, and F.L. Freire, Jr., Appl. Phys. Lett. **60**, 3229 (1992).

[4] S. Mettin, J.H. Kauffman, D.D. Saperstein, J.C. Scott, J. Heyman, and E.E. Haler, J. Mater. Res. **9**, 396 (1994).

[5] D. Li, S. Lopez, Y.W. Chung, M.S. Wong, and W.D. Sproul, J. Vac. Sci. Technol. **13**, 1063 (1995).

[6] D.F. Franceschini, F.L. Freire, Jr., and S.R.P. Silva, Appl. Phys. Lett. **68**, 2645 (1996).

[7] X.-M. He, L. Shu, W.-Z. Li, and H.-D. Li, J. Mater. Res. **12**, 1595 (1997).

[8] V.S. Veerasamy, J. Yuan, G.A.J. Amaratunga, W.I. Milne, K.W.R. Gilkes, M. Weiler, and L.M. Brown, Phys. Rev. B **48**, 17 954 (1993).

[9] F.L. Freire, Jr. and D.F. Franceschini, Thin Solid Films **293**, 236 (1997).

[10] A.Y. Liu and M.L. Cohen, Science **245**, 841 (1989).

[11] R. Priolli, S.I. Zanette, A.O. Caride, D.F. Franceschini, and F.L. Freire, Jr., J. Vac. Sci. Technol. A **14**, 2351 (1996).

[12] A. Stanishevsky, Mater. Lett. **37**, 162 (1998).

[13] S.S. Todorov, D. Marton, K.J. Boyd, A.H. Al Bayati, and J.W. Rabalais, J. Vac. Sci. Technol. A **12**, 3192 (1994).

[14] F.D.A. Aarão Reis and D.F. Franceschini, Appl. Phys. Lett. **74**, 209 (1999).

[15] L.G. Jacobsohn, F.L. Freire, Jr., D.F. Franceschini, M.M. Lacerda, and G. Mariotto, J. Vac. Sci. Technol. A **17**, 545 (1999).

[16] W. Jacob, Thin Solid Films **326**, 1 (1998).

[17] J.M. Kim and J.M. Kosterlitz, Phys. Rev. Lett. **62**, 2289 (1989).

[18] Y. Kim, D.K. Park, and J.M. Kim, J. Phys. A **27**, L533 (1994).

[19] K.J. Clay, S.P. Speakman, G.A.J. Amaratunga, and S.R.P. Silva, J. Appl. Phys. **79**, 7227 (1996).

[20] P. Hammer and W. Gissler, Diamond Relat. Mater. **5**, 1152 (1996).

[21] J. Hong and G. Turban, Diamond Relat. Mater. **8**, 572 (1999).

[22] F. Weich, J. Widani, and T.H. Frauenheim, Phys. Rev. Lett. **78**, 3326 (1997).

[23] J. Krug, Adv. Phys. **46**, 139 (1997).

[24] T. Halpin-Healy and Y.-C. Zhang, Phys. Rep. **254**, 215 (1995).

[25] A.-L. Barabási and H. E. Stanley, *Fractal Concepts in Surface Growth* (Cambridge University Press, New York, 1995).

[26] P. Meakin, Phys. Rep. **235**, 189 (1993).

[27] F. Family and T. Vicsek, J. Phys. A **18**, L75 (1985).

[28] W. Wang and H.A. Cerdeira, Phys. Rev. E **47**, 3357 (1993).

[29] A. von Keudell and W. Moller, J. Appl. Phys. **75**, 7718 (1994).

[30] G.J. Vandentrop, M. Kawasaky, R.M. Nix, I.G. Brown, M. Salmeron, and G.A. Somorjay, Phys. Rev. B **41**, 3200 (1990).

[31] K.-R. Lee, K.Y. Eun, and J.-S. Rhee, Mater. Res. Soc. Symp. Proc. **356**, 233 (1995).

[32] M. Weiler, S. Sattel, T. Giessen, K. Jung, H. Erhardt, V.S. Veerasamy, and J. Robertson, Phys. Rev. B **53**, 1594 (1996).

[33] J.W. Zou, K. Schmidt, K. Reichelt, and B. Dischler, J. Appl. Phys. **67**, 487 (1990).

[34] J.W. Zou, K. Reichelt, K. Schmidt, and B. Dischler, J. Appl. Phys. **65**, 3914 (1989).

[35] M.A. Makeev and A.-L. Barabäsi, Appl. Phys. Lett. **71**, 2800 (1997); **72**, 906 (1998); **73**, 1445 (1998).